

Commun. Theor. Phys. **76** (2024) 015404 (9pp) https://doi.org/10.1088/1572-9494/ad1988

Constraints on the primordial curvature power spectrum by pulsar timing array data: a polynomial parameterization approach

Qin Fei

School of Mathematics and Physics, Hubei Polytechnic University, Huangshi 435003, China

E-mail: feiqin@hbpu.edu.cn

Received 30 October 2023, revised 18 December 2023
Accepted for publication 29 December 2023
Published 23 January 2024

Abstract

The recent stochastic signal observed jointly by NANOGrav, parkes pulsar timing array, European pulsar timing array, and Chinese pulsar timing array can be accounted for by scalar-induced gravitational waves (SIGWs). The source of the SIGWs is from the primordial curvature perturbations, and the main contribution to the SIGWs is from the peak of the primordial curvature power spectrum. To effectively model this peak, we apply the Taylor expansion to parameterize it. With the Taylor expansion parameterization, we apply Bayesian methods to constrain the primordial curvature power spectrum based on the NANOGrav 15 year data set. The constraint on the primordial curvature power spectrum possesses a degree of generality, as the Taylor expansion can effectively approximate a wide range of function profiles.

Keywords: pulsar timing array, scalar-induced gravitational waves, inflation

(Some figures may appear in colour only in the online journal)

1. Introduction

The detection of gravitational waves (GWs) from compact binary mergers [1–3] by LIGO-Virgo-KAGRA has provided valuable insights into the properties of the population of GW sources [4–16]. The next crucial milestone in GW detection is the observation of stochastic GW backgrounds that would provide valuable information about astrophysical and cosmological processes, such as the early universe, dark matter [17–19], and modified gravity [20–24]. Recently, the north American nanohertz observatory for gravitational Waves (NANOGrav) [25, 26], parkes pulsar timing array (PPTA) [27, 28], European pulsar timing array (EPTA) together with Indian pulsar timing array (InPTA) [29, 30], and Chinese pulsar timing array (CPTA) [31], have jointly detected a common-spectrum process exhibiting the Hellings-Downs angular correlation feature inherent in gravitational waves (GWs). Characterized by a fiducial $f^{-2/3}$ characteristic-strain spectrum, this signal is attributed to an ensemble of binary supermassive black hole inspirals, with a strain amplitude of approximately $\sim 10^{-15}$ at a reference frequency of $1\,\mathrm{yr}^{-1}$ [25, 28, 30, 31]. Besides the supermassive black hole binary (SMBHB) scenario, other hypotheses are also proposed [32–55]. Among these hypotheses, scalar-induced gravitational waves (SIGWs) are a strong candidate, offering a more robust explanation than the supermassive black hole binary (SMBHB) model by Bayesian analysis [32, 34]. This paper focuses on exploring the observed PTA signal explained by SIGWs. For further physical processes contributing to the pulsar timing array (PTA) band, please refer to [56–71].

The scalar-induced gravitational waves are induced by the large scalar perturbations seeded from primordial curvature perturbations generated during the inflationary epoch [72–74]. Accompanying the formation of SIGWs, the large scalar perturbations can produce primordial black holes (PBHs) [5, 6, 8, 10, 11, 15, 75–110]. To produce detectable SIGWs, the power spectrum amplitude of primordial curvature perturbations, denoted as $\mathcal{A}_\zeta$, must be on the order of $\mathcal{A}_\zeta \sim \mathcal{O}(0.01)$, while the constraints from cosmic microwave background (CMB) anisotropy observations at large scales are $\mathcal{A}_\zeta = 2.1 \times 10^{-9}$ [111]. Therefore, the significant SIGWs require the power spectrum amplitude of primordial curvature perturbations seven orders of magnitude larger than the constraints at large scales. Generating such a large enhancement

in the primordial curvature power spectrum is hard to achieve in traditional slow-roll inflation models;instead, ultra-slow-roll inflationary scenarios may be able to achieve this purpose [112–154].

The energy density of SIGWs is mainly determined by the peak structure of the primordial curvature power spectrum. In this study, we adopt a polynomial representation to characterize the peak profile of the primordial curvature power spectrum. This polynomial form can be understood as a Taylor expansion capable of effectively describing various peak shapes. By employing this polynomial parameterization, we can derive the most data-favored peak profile of the primordial curvature power spectrum by the Bayes analysis. The organization of this paper is as follows. Section 2 gives the energy density of the SIGWs. Section 3 overviews the parameterization of the primordial curvature power spectrum and presents the constraints on it. Finally, the conclusions are drawn in section 4.

2. The scalar-induced gravitational waves

If the scalar perturbation resulting from the primordial curvature perturbations created during inflation reaches a notable level, the secondary order of linear scalar perturbations may act as a source to induce GWs. In this section, we explore a detailed analysis of the energy density of the SIGWs during the radiation dominated. The perturbed metric within the Newtonian gauge can be expressed as follows:

$$\mathrm{d}s^2 = a^2(\eta)[-(1+2\Phi)\mathrm{d}\eta^2 + \left\{(1-2\Phi)\delta_{ij} + \frac{1}{2}h_{ij}\right\}\mathrm{d}x^i\mathrm{d}x^j]. \tag{1}$$

Here, Φ is the Bardeen potential, and h_{ij} represents the tensor perturbation, satisfying the transverse-traceless gauge condition $\partial^i h_{ij} = h^i_i = 0$. In the Fourier space, the tensor perturbation is denoted by:

$$h_{ij}(\boldsymbol{x},\eta) = \int \frac{\mathrm{d}^3\boldsymbol{k}}{(2\pi)^{3/2}}\mathrm{e}^{\mathrm{i}\boldsymbol{k}\cdot\boldsymbol{x}} \times [h^+_{\boldsymbol{k}}(\eta)e^+_{ij}(\boldsymbol{k}) + h^\times_{\boldsymbol{k}}(\eta)e^\times_{ij}(\boldsymbol{k})], \tag{2}$$

where $e^+_{ij}(\boldsymbol{k})$ and $e^\times_{ij}(\boldsymbol{k})$ are the plus and cross-polarization tensors,

$$e^+_{ij}(\boldsymbol{k}) = \frac{1}{\sqrt{2}}[e_i(\boldsymbol{k})e_j(\boldsymbol{k}) - \bar{e}_i(\boldsymbol{k})\bar{e}_j(\boldsymbol{k})],$$
$$e^\times_{ij}(\boldsymbol{k}) = \frac{1}{\sqrt{2}}[e_i(\boldsymbol{k})\bar{e}_j(\boldsymbol{k}) + \bar{e}_i(\boldsymbol{k})e_j(\boldsymbol{k})]. \tag{3}$$

Here $e_i(\boldsymbol{k})$ and $\bar{e}_i(\boldsymbol{k})$ are the normalized basis vectors orthogonal to the wave vector $\boldsymbol{k}$, with $\boldsymbol{e}\cdot\bar{\boldsymbol{e}} = \boldsymbol{e}\cdot\boldsymbol{k} = \bar{\boldsymbol{e}}\cdot\boldsymbol{k} = 0$.

In Fourier space and neglecting anisotropic stress, the equation of motion for tensor perturbations with either polarization can be expressed as:

$$h''_{\boldsymbol{k}}(\eta) + 2\mathcal{H}h'_{\boldsymbol{k}}(\eta) + k^2h_{\boldsymbol{k}}(\eta) = 4S_{\boldsymbol{k}}(\eta), \tag{4}$$

where η represents the conformal time, $\mathrm{d}\eta = \mathrm{d}t/a$, $\mathcal{H} = a'/a$ is the conformal Hubble parameter. The source term from the linear scalar perturbations is denoted by:

$$S_{\boldsymbol{k}} = \int \frac{\mathrm{d}^3\tilde{\boldsymbol{k}}}{(2\pi)^{3/2}}e_{ij}(\boldsymbol{k})\tilde{k}^i\tilde{k}^j\Big[2\Phi_{\tilde{\boldsymbol{k}}}\Phi_{\boldsymbol{k}-\tilde{\boldsymbol{k}}} + \frac{1}{\mathcal{H}^2}(\Phi'_{\tilde{\boldsymbol{k}}} + \mathcal{H}\Phi_{\tilde{\boldsymbol{k}}})(\Phi'_{\boldsymbol{k}-\tilde{\boldsymbol{k}}} + \mathcal{H}\Phi_{\boldsymbol{k}-\tilde{\boldsymbol{k}}})\Big], \tag{5}$$

where $\Phi_{\boldsymbol{k}}$ denotes the Bardeen potential in the Fourier space, which can be related to the primordial curvature perturbations by

$$\Phi_{\boldsymbol{k}} = \frac{3+3w}{5+3w}T(k\eta)\zeta_{\boldsymbol{k}}, \tag{6}$$

and the transfer function $T(x)$ can be expressed as

$$T(x) = 3\left[\frac{\sin(x/\sqrt{3}) - (x/\sqrt{3})\cos(x/\sqrt{3})}{(x/\sqrt{3})^3}\right]. \tag{7}$$

By using the Green's function method, we can obtain the solution for $h_{\boldsymbol{k}}(\eta)$,

$$h_{\boldsymbol{k}}(\eta) = \frac{4}{a(\eta)}\int^\eta \mathrm{d}\overline{\eta}G_{\boldsymbol{k}}(\eta,\overline{\eta})a(\overline{\eta})S_{\boldsymbol{k}}(\overline{\eta}), \tag{8}$$

with the Green function

$$G_{\boldsymbol{k}}(\eta,\overline{\eta}) = \frac{\sin[k(\eta-\overline{\eta})]}{k}. \tag{9}$$

The definition of the power spectrum of SIGWs, $\mathcal{P}_h$, is

$$\langle h_{\boldsymbol{k}}(\eta)h_{\boldsymbol{p}}(\eta)\rangle = \delta^3(\boldsymbol{k}+\boldsymbol{p})\frac{2\pi^2}{k^3}\mathcal{P}_h(k,\eta). \tag{10}$$

Combining the above relations, we can obtain [72–74, 155–157]

$$\mathcal{P}_h(k,\eta) = 4\int_0^\infty \mathrm{d}v\int_{|1-v|}^{1+v}\mathrm{d}u \times\left[\frac{4v^2-(1-u^2+v^2)^2}{4uv}\right]^2 \times I^2_{\mathrm{RD}}(u,v,x)\mathcal{P}_\zeta(kv)\mathcal{P}_\zeta(ku). \tag{11}$$

Here, the new variables are $u = |\boldsymbol{k}-\tilde{\boldsymbol{k}}|/k$, $v = |\tilde{\boldsymbol{k}}|/k$, $x = k\eta$, and $\mathcal{P}_\zeta$ is the power spectrum of the primordial curvature. Furthermore, we have

$$I_{\mathrm{RD}}(u,v,x) = \int_0^x \mathrm{d}y\, y\sin(x-y)\{3T(uy)T(vy) + y[T(vy)uT'(uy) + vT'(vy)T(uy)] + y^2uvT'(uy)T'(vy)\}. \tag{12}$$

By using the definition of the energy density parameter of GWs

$$\Omega_{\mathrm{GW}}(k,\eta) = \frac{1}{24}\left(\frac{k}{aH}\right)^2\overline{\mathcal{P}_h(k,\eta)}. \tag{13}$$

and equations (11), we can obtain [155, 157]

$$\Omega_{\mathrm{GW}}(k,\eta) = \frac{1}{6}\left(\frac{k}{aH}\right)^2\int_0^\infty \mathrm{d}v\int_{|1-v|}^{1+v}\mathrm{d}u \times\left[\frac{4v^2-(1-u^2+v^2)^2}{4uv}\right]^2 \times I^2_{\mathrm{RD}}(u,v,x)\mathcal{P}_\zeta(kv)\mathcal{P}_\zeta(ku), \tag{14}$$

Table 1. The priors, maximum posterior values, 1-σ credible interval bounds of posteriors for the parameters in the primordial curvature power spectrum parameterization (20) by using NANOGrav 15 years data set and Bayesian methods.

Parameters	$\log_{10}(k_p/\mathrm{Mpc}^{-1})$	$\log_{10}A_0$	$\log_{10}A_2$	$\log_{10}A_3$
prior	$\mathcal{U}(7, 10)$	$\mathcal{U}(-4, 1)$	$\mathcal{U}(-10, 2)$	$\mathcal{U}(-5, 5)$
posterior	$7.75^{+0.68}_{-0.34}$	$-1.63^{+0.75}_{-0.34}$	$-6.74^{+2.98}_{-2.17}$	$-0.07^{+2.63}_{-2.62}$

where $\overline{I^2_{\mathrm{RD}}}$ is the oscillation time average of I^2_{RD}. After the horizon reentry and at late time $x \to \infty$, $\overline{I^2_{\mathrm{RD}}}$ becomes [74]

$$\overline{I^2_{\mathrm{RD}}(v, u, x \to \infty)} = \frac{1}{2x^2}\left(\frac{3(u^2+v^2-3)}{4u^3v^3}\right)^2 \times\{\pi^2(u^2+v^2-3)^2\Theta(v+u-\sqrt{3}) -\left(4uv-(u^2+v^2-3)\ln\left|\frac{3-(u+v)^2}{3-(u-v)^2}\right|\right)^2\}. \quad (15)$$

The evolution of GW energy density is the same as that of radiation. By using this characteristic, we can get the present energy density of GWs:

$$\Omega_{\mathrm{GW}}(k, \eta_0) = \Omega_{r,0}\Omega_{\mathrm{GW}}(k, \eta), \quad (16)$$

where $\Omega_{r,0}$ is the energy density parameter of radiation at present.

3. Methodology and results

The contribution to the energy density of SIGWs is mainly from the peak region of the primordial curvature power spectrum. In this paper, we focus on the peak region of the primordial curvature power spectrum and parameterize it as

$$\log_{10}\mathcal{P}_\zeta(k) = \sum_{i=0}^{n}(\log_{10}A_i)\cdot x^i, \quad -1 < x < 1, \quad (17)$$

where $x = \log_{10}(k/k_p)$, and k_p is the peak scale of primordial curvature power spectrum. The peak can be well described by the polynomial as long as the polynomial term is large enough. The Taylor expansion converges at the condition $|x| < 1$. Because larger polynomial terms will cost larger computing resources, for the sake of simplification, in this paper, we only consider $n = 3$. To ensure that the peak of the power spectrum is located at the scale k_p, the derivatives of power spectrum must satisfy $\mathrm{d}\mathcal{P}_\zeta/\mathrm{d}x = 0$ and $\mathrm{d}^2\mathcal{P}_\zeta/\mathrm{d}x^2 < 0$ at $x = 0$. Furthermore, to ensure that the peak at scale k_p is the only peak, the first derivative should satisfy $\mathrm{d}\mathcal{P}_\zeta/\mathrm{d}x > 0$ for $x < 0$ and $\mathrm{d}\mathcal{P}_\zeta/\mathrm{d}x < 0$ for $x > 0$. For the parameterization considered in this paper, these conditions are equivalent to

$$\log_{10}A_1 = 0, \quad \log_{10}A_2 < -1.5\,|\log_{10}A_3|. \quad (18)$$

For other scales, we use the near-scale-invariance power-law form to parameterize the primordial curvature power spectrum,

$$\mathcal{P}_\zeta(k) = A_*\left(\frac{k}{k_*}\right)^{n_s-1}, \quad x \leqslant -1 \text{ or } x \geqslant 1, \quad (19)$$

where $k_* = 0.05\,\mathrm{Mpc}^{-1}$, $A_* = 2.1\times10^{-9}$, and $n_s = 0.965$ [111]. Therefore, the parameterization is

$$\log_{10}\mathcal{P}_\zeta(k) = \begin{cases}\sum_{i=0}^{n}(\log_{10}A_i)\cdot x^i, & -1 < x < 1,\\ \log_{10}\left[A_*\left(\frac{k}{k_*}\right)^{n_s-1}\right], & x \leqslant -1 \text{ or } x \geqslant 1.\end{cases} \quad (20)$$

There are steps present at $x = -1$ and $x = 1$ in this parameterization. These steps in the power spectrum of the primordial curvature power spectrum can be found in various inflationary mechanisms, such as parametric amplification [86] and sound speed resonance [158]. Hence, the inclusion of steps in the parameterization (20) is considered acceptable. For the parameterization given by (20), when $|x| < 1$, if the spectrum obtained from parameterization (17) is smaller than the spectrum obtained from parameterization (19), we use the latter. In the following, we use the parameterization described by equation (20) and apply Bayesian methods to the NANOGrav 15 years data to obtain the constraint on the amplitude of the primordial curvature power spectrum. Our analysis utilizes data from 14 frequency bins in the NANOGrav 15 year data set [25, 32] to infer the posterior distributions of the parameters in parameterization (20). The computations were performed using the `Bilby` code [159], implementing the `dynesty` algorithm for nested sampling [160]. We formed the log-likelihood function by evaluating the energy density of SIGWs at the 14 specific frequency intervals. Afterward, we computed the sum of the logarithms of probability density functions obtained from 14 independent kernel density estimates [36, 40, 43, 44, 161, 162]. Consequently, we can represent the likelihood function as

$$\ln\mathcal{L}(\Lambda) = \sum_{i=1}^{14}\ln\mathcal{L}_i(\Omega_{\mathrm{GW}}(f_i, \Lambda)), \quad (21)$$

where Λ denotes all the parameters in the parameterization given by equation (20), and the prior for the parameters are listed in table 1. The function $\mathcal{U}$ denotes the uniform distribution. In this study, we incorporate constraints stemming

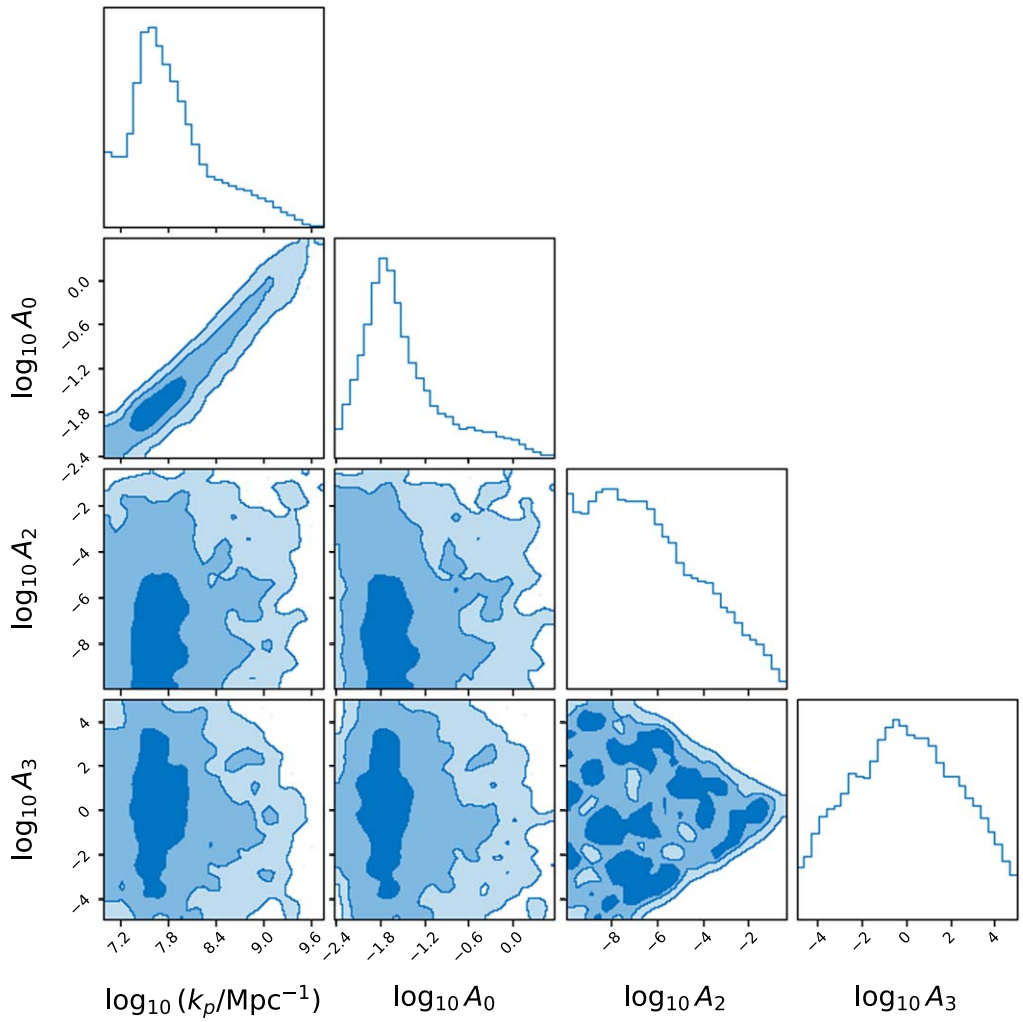

Figure 1. The posterior of the parameters in parameterization (20) using the NANOGrav 15 years data set with Bayesian methods.

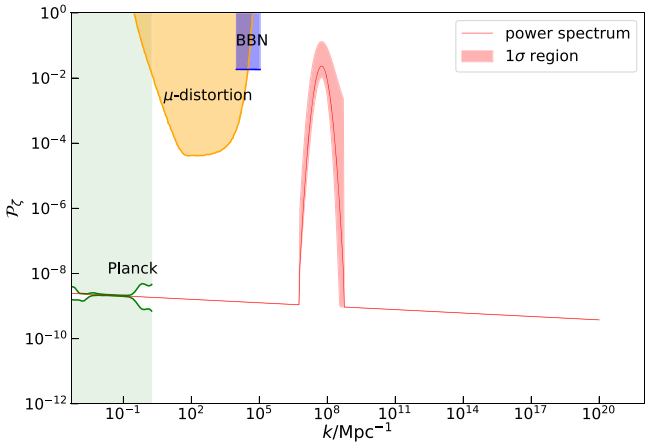

Figure 2. The primordial power spectrum of the parameterization (20) by choosing the 1-σ value listed in table. 1. The green, orange, and blue regions are the constraints from the Planck data [111], μ-distortion of CMB [165], and the effect on the ratio between neutron and proton during the Big Bang nucleosynthesis (BBN) [166], respectively.

from baryon acoustic oscillation and cosmic microwave background (CMB) data [163]. Specifically, we impose a restriction on the integrated energy-density fraction, given by $\int_{k_{\rm min}}^{\infty} h^2\Omega_{\rm GW,0}(k)\, d\ln k \lesssim 2.9\times 10^{-7}$ [164], where $h = H_0/(100\,{\rm km},\ {\rm s}^{-1},\ {\rm Mpc}^{-1}) = 0.674$ [163] is the dimensionless Hubble constant.

The posterior distributions of the parameters in the parameterization (20) are displayed in figure 1, and the maximum posterior values, 1-σ credible interval bounds of posteriors are listed in table 1. The maximum posterior of the peak scale is $k_p = 5.6\times 10^7 {\rm Mpc}^{-1}$, which is consistent with the Gauss model given in the NANOGrav paper [32]. By choosing the values in the 1-σ credible interval bounds of the parameters listed in table 1, we calculate the primordial curvature power spectrum shown in figure 2 and denoted by the red line; the corresponding SIGW are displayed in the figure 3 and denoted by the blue line. Figure 3 shows that the energy density of the SIGWs is consistent with the NANOGrav 15 years data set.

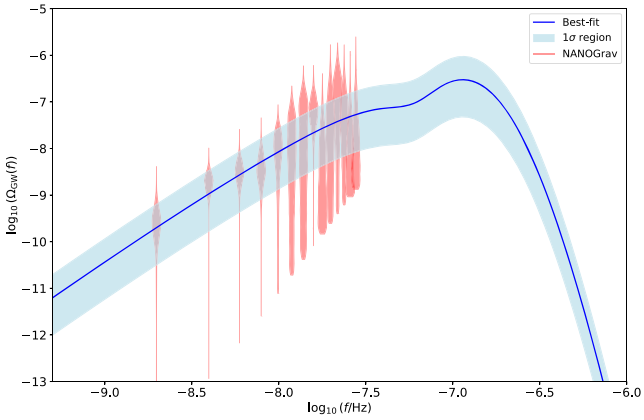

Figure 3. The corresponding energy density of the SIGWs denoted by the blue line. The red violins are the NANOGrav 15 years data set.

4. Conclusion

The stochastic signal detected by the NANOGrav, PPTA, EPTA, and CPTA collaborations can be explained by SIGWs, where the source of the GWs is from the primordial curvature perturbations. The main contribution to the energy density of the SIGWs is from the peak of the primordial curvature power spectrum. In this paper, we focus on the peak region and parameterize the primordial curvature power spectrum near the peak by the Taylor expansion with four terms to characterize the peak behavior. The posterior of the parameters are: $\log_{10}(k_p/\mathrm{Mpc}^{-1}) = 7.75^{+0.68}_{-0.34}$, $\log_{10}A_0 = -1.63^{+0.75}_{-0.34}$, $\log_{10}A_2 = -6.74^{+2.98}_{-2.17}$, $\log_{10}A_3 = -0.07^{+2.63}_{-2.62}$. Because the Taylor expansion can describe most function profiles, our constraint on the primordial curvature power spectrum possesses a degree of generality.

Acknowledgments

This research was supported in part by the National Natural Science Foundation of China under Grant No. 12305060, and the Talent-Introduction Program of Hubei Polytechnic University under Grant No. 19xjk25R.

References

[1] Abbott B P (LIGO Scientific, Virgo) *et al* 2019 GWTC-1: a gravitational-wave transient catalog of compact binary mergers observed by ligo and virgo during the first and second observing runs *Phys. Rev.*X **9** 031040
[2] Abbott R (LIGO Scientific, Virgo) *et al* 2021 GWTC-2: compact binary coalescences observed by ligo and virgo during the first half of the third observing run *Phys. Rev.*X **11** 021053
[3] Abbott R (KAGRA, VIRGO, LIGO Scientific) *et al* 2023 GWTC-3: Compact binary coalescences observed by LIGO and Virgo during the second part of the third observing run *Phys. Rev.*X **13** 041039
[4] Abbott B P (LIGO Scientific, Virgo) *et al* 2019 Binary black hole population properties inferred from the first and second observing runs of advanced LIGO and advanced virgo *Astrophys. J. Lett.* **882** L24
[5] Chen Z C, Huang F and Huang Q G 2019 Stochastic gravitational-wave background from binary black holes and binary neutron stars and implications for LISA *Astrophys. J.* **871** 97
[6] Chen Z C and Huang Q G 2020 Distinguishing primordial black holes from astrophysical black holes by einstein telescope and cosmic explorer *J. Cosmol. Astropart. Phys.* JCAP08(2020)039
[7] Abbott R (LIGO Scientific, Virgo) *et al* 2021 Population properties of compact objects from the second ligo-virgo gravitational-wave transient catalog *Astrophys. J. Lett.* **913** L7
[8] Chen Z C, Yuan C and Huang Q G 2022 Confronting the primordial black hole scenario with the gravitational-wave events detected by LIGO-Virgo *Phys. Lett.* B **829** 137040
[9] Abbott R (KAGRA, VIRGO, LIGO Scientific) *et al* 2023 Population of merging compact binaries inferred using gravitational waves through GWTC-3 *Phys. Rev.*X **13** 011048
[10] Chen Z C, Du S S, Huang Q G and You Z Q 2023 Constraints on primordial-black-hole population and cosmic expansion history from GWTC-3 *J. Cosmol. Astropart. Phys.* JCAP03(2023)024
[11] Liu L, You Z Q, Wu Y and Chen Z C 2023 Constraining the merger history of primordial-black-hole binaries from GWTC-3 *Phys. Rev.* D **107** 063035
[12] Sasaki M, Takhistov V, Vardanyan V and Zhang Y l 2022 Establishing the nonprimordial origin of black hole–neutron star mergers *Astrophys. J.* **931** 2
[13] Kimura R, Suyama T, Yamaguchi M and Zhang Y L 2021 Reconstruction of primordial power spectrum of curvature perturbation from the merger rate of primordial black hole binaries *J. Cosmol. Astropart. Phys.* JCAP04(2021)031
[14] Wang X, Zhang Y l, Kimura R and Yamaguchi M 2023 Reconstruction of power spectrum of primordial curvature perturbations on small scales from primordial black hole binaries scenario of LIGO/VIRGO detection *Sci. China Phys. Mech. Astron.* **66** 260462
[15] Zheng L M, Li Z, Chen Z C, Zhou H and Zhu Z H 2023 Towards a reliable reconstruction of the power spectrum of primordial curvature perturbation on small scales from GWTC-3 *Phys. Lett.* B **838** 137720
[16] You Z Q, Chen Z C, Liu L, Yi Z, Liu X J, Wu Y and Gong Y 2023 Constraints on peculiar velocity distribution of binary black holes using gravitational waves with GWTC-3 arXiv:2306.12950
[17] Wei H, Chen Z C and Liu J 2013 Cosmological constraints on variable warm dark matter *Phys. Lett.* B **720** 271–6
[18] Wei H, Liu J, Chen Z C and Yan X P 2013 Indistinguishability of warm dark matter, modified gravity, and coupled cold dark matter *Phys. Rev.* D **88** 043510
[19] Du S S, Wei J J, You Z Q, Chen Z C, Zhu Z H and Liang E W 2023 Model-independent determination of H0 and Ω K, 0 using time-delay galaxy lenses and gamma-ray bursts *Mon. Not. Roy. Astron. Soc.* **521** 4963–75
[20] Chen Z C, Wu Y and Wei H 2015 Post-newtonian approximation of teleparallel gravity coupled with a scalar field *Nucl. Phys.* B **894** 422–38
[21] Wu Y, Chen Z C, Wang J and Wei H 2015 $f(T)$ nonlinear massive gravity and the cosmic acceleration *Commun. Theor. Phys.* **63** 701–8
[22] Huang Y, Gong Y, Liang D and Yi Z 2015 Thermodynamics of scalar–tensor theory with non-minimally derivative coupling *Eur. Phys. J.* C **75** 351
[23] Zhu Y and Gong Y 2016 PPN parameters in gravitational theory with nonminimally derivative coupling *Int. J. Mod. Phys.* D **26** 1750005

[24] Gong Y, Papantonopoulos E and Yi Z 2018 Constraints on scalar–tensor theory of gravity by the recent observational results on gravitational waves *Eur. Phys. J.* C **78** 738
[25] Agazie G (NANOGrav) *et al* 2023 The NANOGrav 15 year data set: evidence for a gravitational-wave background *Astrophys. J. Lett.* **951** L8 The NANOGrav 15 yr year data set: evidence for a gravitational-wave background
[26] Agazie G (NANOGrav) *et al* 2023 The NANOGrav 15 year data set: observations and timing of 68 millisecond pulsars *Astrophys. J. Lett.* **951** L9 The NANOGrav 15 yr year data set: observations and timing of 68 millisecond pulsars
[27] Zic A *et al* 2023 The parkes pulsar timing array third data release arXiv:2306.16230
[28] Reardon D J *et al* 2023 Search for an isotropic gravitational-wave background with the parkes pulsar timing array *Astrophys. J. Lett.* **951** L6
[29] Antoniadis J (EPTA) *et al* 2023 The second data release from the European Pulsar Timing Array—I. The dataset and timing analysis *Astron. Astrophys.* **678** A48
[30] Antoniadis J (EPTA, InPTA) *et al* 2023 The second data release from the European pulsar timing array: III. Search for gravitational wave signals *Astron. Astrophys.* **678** A50
[31] Xu H *et al* 2023 Searching for the nano-hertz stochastic gravitational wave background with the Chinese pulsar timing array data release I *Astron. Astrophys.* **23** 075024
[32] Afzal A (NANOGrav) *et al* 2023 The NANOGrav 15 year data set: search for signals from new physics *Astrophys. J. Lett.* **951** L11 The NANOGrav 15 yr year data set: search for signals from new physics
[33] Antoniadis J (EPTA) *et al* 2023 The second data release from the European pulsar timing array: V. Implications for massive black holes, dark matter and the early Universe arXiv:2306.16227
[34] Yi Z, Gao Q, Gong Y, Wang Y and Zhang F 2023 Scalar induced gravitational waves in light of Pulsar Timing Array data *Sci. China Phys. Mech. Astron.* **66** 120404
[35] Franciolini G, Iovino A Jr., Vaskonen V and Veermae H 2023 Recent gravitational wave observation by pulsar timing arrays and primordial black holes: the importance of non-gaussianities *Phys. Rev. Lett.* **131** 201401
[36] Liu L, Chen Z C and Huang Q G 2023 Implications for the non-Gaussianity of curvature perturbation from pulsar timing arrays arXiv:2307.01102
[37] Vagnozzi S 2023 Inflationary interpretation of the stochastic gravitational wave background signal detected by pulsar timing array experiments *J. High Energ. Astrophys.* **39** 81–98
[38] Cai Y F, He X C, Ma X H, Yan S F and Yuan G W 2023 Limits on scalar-induced gravitational waves from the stochastic background by pulsar timing array observations *Sci. Bull.* **68** 2929–35
[39] Bi Y C, Wu Y M, Chen Z C and Huang Q G 2023 Implications for the supermassive black hole binaries from the NANOGrav 15 year data set *Sci. China Phys. Mech. Astron.* **66** 120402
[40] Wu Y M, Chen Z C and Huang Q G 2023 Cosmological interpretation for the stochastic signal in pulsar timing arrays arXiv:2307.03141
[41] Franciolini G, Racco D and Rompineve F 2023 Footprints of the QCD crossover on cosmological gravitational waves at pulsar timing arrays arXiv:2306.17136
[42] You Z Q, Yi Z and Wu Y 2023 Constraints on primordial curvature power spectrum with pulsar timing arrays *J. Cosmol. Astropart. Phys.* JCAP11(2023)065
[43] Jin J H, Chen Z C, Yi Z, You Z Q, Liu L and Wu Y 2023 Confronting sound speed resonance with pulsar timing arrays *J. Cosmol. Astropart. Phys.* JCAP09(2023)016
[44] Liu L, Chen Z C and Huang Q G 2023 Probing the equation of state of the early Universe with pulsar timing arrays *J. Cosmol. Astropart. Phys.* JCAP11(2023)071
[45] An H, Su B, Tai H, Wang L T and Yang C 2023 Phase transition during inflation and the gravitational wave signal at pulsar timing arrays arXiv:2308.00070
[46] Zhang Z, Cai C, Su Y H, Wang S, Yu Z H and Zhang H H 2023 Nano-Hertz gravitational waves from collapsing domain walls associated with freeze-in dark matter in light of pulsar timing array observations *Phys. Rev.* D **108** 095037
[47] Das B, Jaman N and Sami M 2023 Gravitational wave background from quintessential inflation and NANOGrav data *Phys. Rev.* D **108** 103510
[48] Balaji S, Domènech G and Franciolini G 2023 Scalar-induced gravitational wave interpretation of PTA data: the role of scalar fluctuation propagation speed *J. Cosmol. Astropart. Phys.* JCAP10(2023)041
[49] Du X K, Huang M X, Wang F and Zhang Y K 2023 Did the nHZ gravitational waves signatures observed by nanograv indicate multiple sector susy breaking? arXiv:2307.02938
[50] Oikonomou V K 2023 Flat energy spectrum of primordial gravitational waves versus peaks and the NANOGrav 2023 observation *Phys. Rev.* D **108** 043516
[51] Yi Z, You Z Q, Wu Y, Chen Z C and Liu L 2023 Exploring the NANOGrav signal and planet-mass primordial black holes through Higgs inflation arXiv:2308.14688
[52] Yi Z, You Z Q and Wu Y 2023 Model-independent reconstruction of the primordial curvature power spectrum from PTA data arXiv:2308.05632
[53] Chen Z C, Huang Q G, Liu C, Liu L, Liu X J, Wu Y, Wu Y M, Yi Z and You Z Q 2023 Prospects for Taiji to detect a gravitational-wave background from cosmic strings arXiv:2310.00411
[54] Liu L, Wu Y and Chen Z C 2023 Simultaneously probing the sound speed and equation of state of the early Universe with pulsar timing arrays arXiv:2310.16500
[55] Guo S Y, Khlopov M, Liu X, Wu L, Wu Y and Zhu B 2023 Footprints of axion-like particle in pulsar timing array data and JWST observations arXiv:2306.17022
[56] Zhu X J, Cui W and Thrane E 2019 The minimum and maximum gravitational-wave background from supermassive binary black holes *Mon. Not. Roy. Astron. Soc.* **482** 2588–96
[57] Li J, Chen Z C and Huang Q G 2019 Measuring the tilt of primordial gravitational-wave power spectrum from observations *Sci. China Phys. Mech. Astron.* **62** 110421
LI J, Chen Z C and Haung Q G 2021 *Sci. China Phys. Mech. Astron.* **64** 250451
[58] Chen Z C, Yuan C and Huang Q G 2021 Non-tensorial gravitational wave background in NANOGrav 12.5 year data set *Sci. China Phys. Mech. Astron.* **64** 120412
[59] Wu Y M, Chen Z C and Huang Q G 2022 Constraining the polarization of gravitational waves with the parkes pulsar timing array second data release *Astrophys. J.* **925** 37
[60] Chen Z C, Wu Y M and Huang Q G 2022 Searching for isotropic stochastic gravitational-wave background in the international pulsar timing array second data release *Commun. Theor. Phys.* **74** 105402
[61] Chen Z C, Wu Y M and Huang Q G 2022 Search for the gravitational-wave background from cosmic strings with the parkes pulsar timing array second data release *Astrophys. J.* **936** 20
[62] Wu Y M, Chen Z C, Huang Q G, Zhu X, Bhat N D R, Feng Y, Hobbs G, Manchester R N, Russell C J and Shannon R M 2022 Constraining ultralight vector dark matter with the Parkes Pulsar Timing Array second data release *Phys. Rev.* D **106** L081101
[63] Falxa M (IPTA) *et al* 2023 Searching for continuous gravitational waves in the second data release of the

international pulsar timing array *Mon. Not. Roy. Astron. Soc.* **521** 5077–86
[64] Wu Y M, Chen Z C and Huang Q G 2023 Search for stochastic gravitational-wave background from massive gravity in the NANOGrav 12.5 year dataset *Phys. Rev.* D **107** 042003
[65] Wu Y M, Chen Z C and Huang Q G 2023 Pulsar timing residual induced by ultralight tensor dark matter *J. Cosmol. Astropart. Phys.* JCAP09(2023)021
[66] Agazie G (International Pulsar Timing Array) *et al* 2023 Comparing recent PTA results on the nanohertz stochastic gravitational wave background arXiv:2309.00693
[67] Wu Y M, Chen Z C, Bi Y C and Huang Q G 2023 Constraining the graviton mass with the NANOGrav 15 year data set arXiv:2310.07469
[68] Bi Y C, Wu Y M, Chen Z C and Huang Q G 2023 Constraints on the velocity of gravitational waves from NANOGrav 15 year data set arXiv:2310.08366
[69] Chen Z C, Wu Y M, Bi Y C and Huang Q G 2023 Search for non-tensorial gravitational-wave backgrounds in the NANOGrav 15 year data set arXiv:2310.11238
[70] Chen Z C, Li S L, Wu P and Yu H 2023 NANOGrav hints for first-order confinement-deconfinement phase transition in different QCD-matter scenarios arXiv:2312.01824
[71] Wang Z, Lei L, Jiao H, Feng L and Fan Y Z 2023 The nanohertz stochastic gravitational wave background from cosmic string loops and the abundant high redshift massive galaxies *Sci. China Phys. Mech. Astron.* **66** 120403
[72] Ananda K N, Clarkson C and Wands D 2007 The Cosmological gravitational wave background from primordial density perturbations *Phys. Rev.* D **75** 123518
[73] Baumann D, Steinhardt P J, Takahashi K and Ichiki K 2007 Gravitational wave spectrum induced by primordial scalar perturbations *Phys. Rev.* D **76** 084019
[74] Kohri K and Terada T 2018 Semianalytic calculation of gravitational wave spectrum nonlinearly induced from primordial curvature perturbations *Phys. Rev.* D **97** 123532
[75] Hawking S 1971 Gravitationally collapsed objects of very low mass *Mon. Not. Roy. Astron. Soc.* **152** 75
[76] Carr B J and Hawking S W 1974 Black holes in the early Universe *Mon. Not. Roy. Astron. Soc.* **168** 399–415
[77] Saito R and Yokoyama J 2009 Gravitational wave background as a probe of the primordial black hole abundance *Phys. Rev. Lett.* **102** 161101
Saito R and Yokoyama J 2011 *Phys. Rev. Lett.* **107** 069901
[78] Alabidi L, Kohri K, Sasaki M and Sendouda Y 2012 Observable spectra of induced gravitational waves from inflation *J. Cosmol. Astropart. Phys.* JCAP09(2012)017
[79] Sasaki M, Suyama T, Tanaka T and Yokoyama S 2018 Primordial black holes—perspectives in gravitational wave astronomy *Class. Quant. Grav.* **35** 063001
[80] Nakama T, Silk J and Kamionkowski M 2017 Stochastic gravitational waves associated with the formation of primordial black holes *Phys. Rev.* D **95** 043511
[81] Di H and Gong Y 2018 Primordial black holes and second order gravitational waves from ultra-slow-roll inflation *J. Cosmol. Astropart. Phys.* JCAP07(2018)007
[82] Cheng S L, Lee W and Ng K W 2018 Primordial black holes and associated gravitational waves in axion monodromy inflation *J. Cosmol. Astropart. Phys.* JCAP07(2018)001
[83] Cai R G, Pi S, Wang S J and Yang X Y 2019 Resonant multiple peaks in the induced gravitational waves *J. Cosmol. Astropart. Phys.* JCAP05(2019)013
[84] Cai R g, Pi S and Sasaki M 2019 Gravitational waves induced by non-gaussian scalar perturbations *Phys. Rev. Lett.* **122** 201101
[85] Cai R G, Pi S, Wang S J and Yang X Y 2019 Pulsar timing array constraints on the induced gravitational waves *J. Cosmol. Astropart. Phys.* JCAP10(2019)059
[86] Cai R G, Guo Z K, Liu J, Liu L and Yang X Y 2020 Primordial black holes and gravitational waves from parametric amplification of curvature perturbations *J. Cosmol. Astropart. Phys.* JCAP06(2020)013
[87] Wu Y 2020 Merger history of primordial black-hole binaries *Phys. Rev.* D **101** 083008
[88] Cai R G, Ding Y C, Yang X Y and Zhou Y F 2021 Constraints on a mixed model of dark matter particles and primordial black holes from the galactic 511 keV line *J. Cosmol. Astropart. Phys.* JCAP03(2021)057
[89] Pi S and Sasaki M 2020 Gravitational waves induced by scalar perturbations with a lognormal peak *J. Cosmol. Astropart. Phys.* JCAP09(2020)037
[90] Domènech G, Pi S and Sasaki M 2020 Induced gravitational waves as a probe of thermal history of the universe *J. Cosmol. Astropart. Phys.* JCAP08(2020)017
[91] Liu L, Guo Z K and Cai R G 2019 Effects of the surrounding primordial black holes on the merger rate of primordial black hole binaries *Phys. Rev.* D **99** 063523
[92] Liu L, Guo Z K and Cai R G 2019 Effects of the merger history on the merger rate density of primordial black hole binaries *Eur. Phys. J.* C **79** 717
[93] Liu L, Guo Z K, Cai R G and Kim S P 2020 Merger rate distribution of primordial black hole binaries with electric charges *Phys. Rev.* D **102** 043508
[94] Liu L, Yang X Y, Guo Z K and Cai R G 2023 Testing primordial black hole and measuring the Hubble constant with multiband gravitational-wave observations *J. Cosmol. Astropart. Phys.* JCAP01(2023)006
[95] Chen Z C, Yuan C and Huang Q G 2020 Pulsar timing array constraints on Primordial black holes with NANOGrav 11 year dataset *Phys. Rev. Lett.* **124** 251101
[96] Yuan C, Chen Z C and Huang Q G 2020 Scalar induced gravitational waves in different gauges *Phys. Rev.* D **101** 063018
[97] Yuan C, Chen Z C and Huang Q G 2020 Log-dependent slope of scalar induced gravitational waves in the infrared regions *Phys. Rev.* D **101** 043019
[98] Yuan C, Chen Z C and Huang Q G 2019 Probing primordial–black-hole dark matter with scalar induced gravitational waves *Phys. Rev.* D **100** 081301
[99] Carr B, Kohri K, Sendouda Y and Yokoyama J 2021 Constraints on primordial black holes *Rept. Prog. Phys.* **84** 116902
[100] Liu L, Christiansen O, Guo Z K, Cai R G and Kim S P 2020 Gravitational and electromagnetic radiation from binary black holes with electric and magnetic charges: circular orbits on a cone *Phys. Rev.* D **102** 103520
[101] Liu L, Christiansen O, Ruan W H, Guo Z K, Cai R G and Kim S P 2021 Gravitational and electromagnetic radiation from binary black holes with electric and magnetic charges: elliptical orbits on a cone *Eur. Phys. J.* C **81** 1048
[102] Yi Z and Fei Q 2023 Constraints on primordial curvature spectrum from primordial black holes and scalar-induced gravitational waves *Eur. Phys. J.* C **83** 82
[103] Papanikolaou T, Tzerefos C, Basilakos S and Saridakis E N 2022 Scalar induced gravitational waves from primordial black hole Poisson fluctuations in f(R) gravity *J. Cosmol. Astropart. Phys.* JCAP10(2022)013
[104] Papanikolaou T, Tzerefos C, Basilakos S and Saridakis E N 2023 No constraints for f(T) gravity from gravitational waves induced from primordial black hole fluctuations *Eur. Phys. J.* C **83** 31
[105] Chakraborty A, Chanda P K, Pandey K L and Das S 2022 Formation and abundance of late-forming primordial black holes as dark matter *Astrophys. J.* **932** 119
[106] Liu L and Kim S P 2022 Gravitational and electromagnetic radiations from binary black holes with electric and magnetic charges *17th Italian-Korean Symp. on Relativistic Astrophysics*

[107] Chen Z C and Huang Q G 2018 Merger rate distribution of primordial-black-hole binaries *Astrophys. J.* **864** 61
[108] Liu L and Kim S P 2022 Merger rate of charged black holes from the two-body dynamical capture *J. Cosmol. Astropart. Phys.* JCAP03(2022)059
[109] Chen Z C, Kim S P and Liu L 2023 Gravitational and electromagnetic radiation from binary black holes with electric and magnetic charges: hyperbolic orbits on a cone *Commun. Theor. Phys.* **75** 065401
[110] Meng D S, Yuan C and Huang Q G 2023 Primordial black holes generated by the non-minimal spectator field *Sci. China Phys. Mech. Astron.* **66** 280411
[111] Akrami Y (Planck) *et al* 2020 Planck 2018 results: X. Constraints on inflation *Astron. Astrophys.* **641** A10
[112] Martin J, Motohashi H and Suyama T 2013 Ultra slow-roll inflation and the non-gaussianity consistency relation *Phys. Rev.* D **87** 023514
[113] Motohashi H, Starobinsky A A and Yokoyama J 2015 Inflation with a constant rate of roll *J. Cosmol. Astropart. Phys.* JCAP09(2015)018
[114] Yi Z and Gong Y 2018 On the constant-roll inflation *J. Cosmol. Astropart. Phys.* JCAP03(2018)052
[115] Yi Z and Gong Y 2016 Nonminimal coupling and inflationary attractors *Phys. Rev.* D **94** 103527
[116] Fei Q, Gong Y, Lin J and Yi Z 2017 The reconstruction of tachyon inflationary potentials *J. Cosmol. Astropart. Phys.* JCAP08(2017)018
[117] Garcia-Bellido J and Ruiz Morales E 2017 Primordial black holes from single field models of inflation *Phys. Dark Univ.* **18** 47–54
[118] Germani C and Prokopec T 2017 On primordial black holes from an inflection point *Phys. Dark Univ.* **18** 6–10
[119] Motohashi H and Hu W 2017 Primordial black holes and slow-roll violation *Phys. Rev.* D **96** 063503
[120] Ezquiaga J M, Garcia-Bellido J and Ruiz Morales E 2018 Primordial black hole production in critical higgs inflation *Phys. Lett.* B **776** 345–9
[121] Di H and Gong Y 2018 Primordial black holes and second order gravitational waves from ultra-slow-roll inflation *J. Cosmol. Astropart. Phys.* JCAP07(2018)007
[122] Yi Z and Gong Y 2019 Gauss–Bonnet inflation and the string swampland *Universe* **5** 200
[123] Yi Z, Gong Y and Sabir M 2018 Inflation with Gauss–Bonnet coupling *Phys. Rev.* D **98** 083521
[124] Ballesteros G, Beltran Jimenez J and Pieroni M 2019 Black hole formation from a general quadratic action for inflationary primordial fluctuations *J. Cosmol. Astropart. Phys.* JCAP06(2019)016
[125] Dalianis I, Kehagias A and Tringas G 2019 Primordial black holes from α-attractors *J. Cosmol. Astropart. Phys.* JCAP01(2019)037
[126] Bezrukov F, Pauly M and Rubio J 2018 On the robustness of the primordial power spectrum in renormalized Higgs inflation *J. Cosmol. Astropart. Phys.* JCAP02(2018)040
[127] Kannike K, Marzola L, Raidal M and Veermäe H 2017 Single field double inflation and primordial black holes *J. Cosmol. Astropart. Phys.* JCAP09(2017)020
[128] Fei Q, Yi Z and Yang Y 2020 The reconstruction of non-minimal derivative coupling inflationary potentials *Universe* **6** 213
[129] Lin J, Gao Q, Gong Y, Lu Y, Zhang C and Zhang F 2020 Primordial black holes and secondary gravitational waves from k and G inflation *Phys. Rev.* D **101** 103515
[130] Lin J, Gao S, Gong Y, Lu Y, Wang Z and Zhang F 2023 Primordial black holes and scalar induced gravitational waves from Higgs inflation with noncanonical kinetic term *Phys. Rev.* D **107** 043517
[131] Yi Z and Zhu Z H 2021 Inflationary attractors from a non-canonical kinetic term arXiv:2106.10303
[132] Gao Q, Gong Y and Yi Z 2021 Primordial black holes and secondary gravitational waves from natural inflation *Nucl. Phys.* B **969** 115480
[133] Gao Q, Gong Y and Yi Z 2019 On the constant-roll inflation with large and small η_H *Universe* **5** 215
[134] Gao Q 2021 Primordial black holes and secondary gravitational waves from chaotic inflation *Sci. China Phys. Mech. Astron.* **64** 280411
[135] Yi Z, Gong Y, Wang B and Zhu Z h 2021 Primordial black holes and secondary gravitational waves from the Higgs field *Phys. Rev.* D **103** 063535
[136] Yi Z, Gao Q, Gong Y and Zhu Z h 2021 Primordial black holes and scalar-induced secondary gravitational waves from inflationary models with a noncanonical kinetic term *Phys. Rev.* D **103** 063534
[137] Yi Z and Zhu Z H 2022 NANOGrav signal and LIGO-Virgo primordial black holes from the Higgs field *J. Cosmol. Astropart. Phys.* JCAP05(2022)046
[138] Yi Z 2023 Primordial black holes and scalar-induced gravitational waves from the generalized Brans-Dicke theory *J. Cosmol. Astropart. Phys.* JCAP03(2023)048
[139] Zhang F, Gong Y, Lin J, Lu Y and Yi Z 2021 Primordial non-Gaussianity from G-inflation *J. Cosmol. Astropart. Phys.* JCAP04(2021)045
[140] Pi S, Zhang Y l, Huang Q G and Sasaki M 2018 Scalaron from R^2-gravity as a heavy field *J. Cosmol. Astropart. Phys.* JCAP05(2018)042
[141] Kamenshchik A Y, Tronconi A, Vardanyan T and Venturi G 2019 Non-canonical inflation and primordial black holes production *Phys. Lett.* B **791** 201–5
[142] Fu C, Wu P and Yu H 2019 Primordial black holes from inflation with nonminimal derivative coupling *Phys. Rev.* D **100** 063532
[143] Fu C, Wu P and Yu H 2020 Scalar induced gravitational waves in inflation with gravitationally enhanced friction *Phys. Rev.* D **101** 023529
[144] Dalianis I, Karydas S and Papantonopoulos E 2020 Generalized non-minimal derivative coupling: application to inflation and primordial black hole production *J. Cosmol. Astropart. Phys.* JCAP06(2020)040
[145] Gundhi A and Steinwachs C F 2021 Scalaron–Higgs inflation reloaded: Higgs-dependent scalaron mass and primordial black hole dark matter *Eur. Phys. J.* C **81** 460
[146] Cheong D Y, Lee S M and Park S C 2021 Primordial black holes in Higgs-R^2 inflation as the whole of dark matter *J. Cosmol. Astropart. Phys.* JCAP01(2021)032
[147] Zhang F 2022 Primordial black holes and scalar induced gravitational waves from the E model with a Gauss-Bonnet term *Phys. Rev.* D **105** 063539
[148] Zhang F, Lin J and Lu Y 2021 Double-peaked inflation model: scalar induced gravitational waves and primordial-black-hole suppression from primordial non-Gaussianity *Phys. Rev.*D **104** 063515
Zhang F, Lin J and Lu Y 2021 *Phys. Rev.*D **104** 129902
[149] Kawai S and Kim J 2021 Primordial black holes from Gauss-Bonnet-corrected single field inflation *Phys. Rev.* D **104** 083545
[150] Cai R G, Chen C and Fu C 2021 Primordial black holes and stochastic gravitational wave background from inflation with a noncanonical spectator field *Phys. Rev.* D **104** 083537
[151] Chen P, Koh S and Tumurtushaa G 2021 Primordial black holes and induced gravitational waves from inflation in the Horndeski theory of gravity arXiv:2107.08638
[152] Karam A, Koivunen N, Tomberg E, Vaskonen V and Veermäe H 2023 Anatomy of single-field inflationary models for primordial black holes *J. Cosmol. Astropart. Phys.* JCAP03(2023)013
[153] Ashoorioon A, Rostami A and Firouzjaee J T 2021 EFT compatible PBHs: effective spawning of the seeds for

primordial black holes during inflation *J. High Energy Phys.* JHEP07(2021)087
[154] Garcia-Saenz S, Lu Y and Shuai Z 2023 Scalar-induced gravitational waves from ghost inflation and parity violation *Phys. Rev.* D **108** 123507
[155] Lu Y, Gong Y, Yi Z and Zhang F 2019 Constraints on primordial curvature perturbations from primordial black hole dark matter and secondary gravitational waves *J. Cosmol. Astropart. Phys.* JCAP12(2019)031
[156] Inomata K, Kawasaki M, Mukaida K, Tada Y and Yanagida T T 2017 Inflationary primordial black holes for the LIGO gravitational wave events and pulsar timing array experiments *Phys. Rev.* D **95** 123510
[157] Espinosa J R, Racco D and Riotto A 2018 A cosmological signature of the sm higgs instability: gravitational waves *J. Cosmol. Astropart. Phys.* JCAP09(2018)012
[158] Cai Y F, Tong X, Wang D G and Yan S F 2018 Primordial black holes from sound speed resonance during inflation *Phys. Rev. Lett.* **121** 081306
[159] Ashton G *et al* 2019 BILBY: a user-friendly Bayesian inference library for gravitational-wave astronomy *Astrophys. J. Suppl.* **241** 27
[160] Skilling J N S 2004 *AIP Conf. Proc.* **735** 395–405
[161] Moore C J and Vecchio A 2021 Ultra-low-frequency gravitational waves from cosmological and astrophysical processes *Nat. Astron.* **5** 1268–74
[162] Lamb W G, Taylor S R and van Haasteren R 2023 Rapid refitting techniques for Bayesian spectral characterization of the gravitational wave background using pulsar timing arrays *Phys. Rev.* D **108** 103019
[163] Aghanim N (Planck) *et al* 2020 Planck 2018 results: VI. Cosmological parameters *Astron. Astrophys.* **641** A6 [Erratum: Astron.Astrophys. 652, C4 (2021)]
Aghanim *et al* 2021 *Astron. Astrophys.* **652** C4
[164] Clarke T J, Copeland E J and Moss A 2020 Constraints on primordial gravitational waves from the cosmic microwave background *J. Cosmol. Astropart. Phys.* JCAP10(2020)002
[165] Fixsen D J, Cheng E S, Gales J M, Mather J C, Shafer R A and Wright E L 1996 The cosmic microwave background spectrum from the full COBE FIRAS data set *Astrophys. J.* **473** 576
[166] Inomata K, Kawasaki M and Tada Y 2016 Revisiting constraints on small scale perturbations from big-bang nucleosynthesis *Phys. Rev.* D **94** 043527